OPEN

Oncogene (2014) 33, 5193–5200

www.nature.com/onc

ORIGINAL ARTICLE

Loss of presenilin 2 is associated with increased iPLA2 activity and lung tumor development

H-M Yun[1,6], MH Park[1,6], DH Kim[1], YJ Ahn[1], K-R Park[1], TM Kim[2], NY Yun[1], YS Jung[3], DY Hwang[4], DY Yoon[5], SB Han[1] and JT Hong[1]

Presenilins are the enzymatic components of γ-secretase complex that cleaves amyloid precursor protein, Notch and β-catenin, which has critical roles in the development of Alzheimer's disease and cancer cell growth. Therefore, in the present study, we studied the effects and mechanisms of PS2 knockout on lung cancer development and possible mechanisms as a key regulator of lung tumor development. We compared carcinogen-induced tumor growth between PS2 knockout mice and wild-type mice. PS2 knockout mice showed increased urethane (1 mg/g)-induced lung tumor incidence when compared with that of wild-type mice with decreased activity of γ-secretase in the lung tumor tissues. Consequently, iPLA2 activities in lung tumor tissues of PS2 knockout mice were much higher than in tumor tissues of wild-type mice. Furthermore, knockdown of PS2 using PS2 siRNA decreased γ-secretase activity with increased iPLA2 activity in the lung cancer cells (A549 and NCI-H460), leading to increased lung cancer cell growth. PS2 knockout mice and PS2 knockdown lung cancer cells showed increased DNA-binding activities of nuclear factor kappa-beta, signal transducer and activator of transcription 3 (STAT3) and AP-1 which are critical transcriptional factors of iPLA2 than those of PS2 wild-type mice and control lung cancer cells. Taken together, these results suggest that the loss of PS2 could have a critical role in lung tumor development through the upregulation of iPLA2 activity by reducing γ-secretase.

Oncogene (2014) **33,** 5193–5200; doi:10.1038/onc.2014.128; published online 26 May 2014

INTRODUCTION

Presenilins (PSs) have two homologs, PS1 and PS2, and function as the catalytic subunits of γ-secretase.[1,2] γ-secretase, an aspartyl protease complex in cell membrane, contains a key subunit, PS. They are the enzymic components that cleave more than 30 substrates, and produce as well as translocate intracellular domains of those substrates in nucleus.[3–5] Most cleavages are transmembrane signals or proteins such as β-amyloid precursor protein (APP), Notch, cadherins, CD44 and so on,[5,6] which contain the GxxxG pentapeptide in their transmembrane domain.[7] PS/γ-secretase-dependent cleavages and translocation into nucleus of oncoproteins such as notch, amyloid precursor protein intracellular domain, vascular endothelial growth factor receptor, E-cadherin, CD44 and ErbB are involved in the growth of leukemia cancer, glioma, colon cancer and breast cancer.[8–12] Presenilins have important roles in cell survival and tumorigenesis.[13–15] It was reported that skin tumorigenesis was higher in PS1 knockout mice,[16] and carcinogen-induced brain tumor incidence was also higher in PS1-mutant mice.[17] Germline mutations of PS2 (R62H and R71W) induced breast cancer growth,[18] and also reported that PS 1 is frequently overexpressed and positively associated with epidermal growth factor receptor expression in head and neck squamous cell carcinoma.[19] However, other studies have shown opposite results. Presenilin-1 mutation induced the activation of caspase-3 in human neuroglioma cells.[20] Presenilin-1 exon 9 deletion and L250S mutations sensitize SH-SY5Y neuroblastoma cells to hyperosmotic stress-induced apoptosis.[21] Glioma cell growth and invasion were prevented by the inhibition of PS2.[10] A recent epidemiological study demonstrated that older adults with prevalent clinical Alzheimer's disease developed cancer at a slower rate compared with older adults without Alzheimer's disease.[22] In addition, we observed that spontaneous lung tumor incidence was much lower in the PS2 (N141I)-mutant mice (unpublished data). Thus, critical relevance between PS and tumor development are controversial and possible mechanisms are not yet clarified.

Lung cancer is a lethal disease and continues to be the leading cause of cancer-related mortality worldwide.[23] Although smoking is the primary cause of most lung cancer cases, approximately 10–15% are caused by genetics.[24] In the non-small cell lung cancers, the proliferation and apoptosis of cancer cells are regulated by several signal transduction pathways. Proteomics analysis suggests that the expression of peroxiredoxins (PRDXs), proliferating cell nuclear antigen (PCNA), interleukin-6 (IL-6) and activator protein-1 (AP-1) were increased, while that of tumor necrosis factor receptor was decreased in lung cancer cell lines and human lung tumor tissues.[25–27] PRDXs, thiol-specific antioxidant proteins having six isoforms (PRDX1 ~ PRDX6) are expressed in mammals, yeast and bacteria. PRDXs are classified based on having either one (1-Cys) or two (2-Cys) conserved cysteine residues,[28] and they may have important roles in both lung tumor progression and resistance.[29,30] Among the six members, PRDX6 is the only peroxiredoxin having both phospholipase A2 (PLA2) and glutathione peroxidase activities.[31] PRDX6 is elevated in several lung diseases including lung cancer, mesothelioma and

[1]College of Pharmacy and Medical Research Center, Chungbuk National University, Gaeshin-dong, Heungduk-gu, Cheongju, Chungbuk, Republic of Korea; [2]College of Veterinary Medicine, Chungbuk National University, 12, Gaeshin-dong, Heungduk-gu, Cheongju, Chungbuk, Republic of Korea; [3]College of Pharmacy, Pusan National University, San 30, Jangjeon-dong, Geumjeung-gu, Busan, Republic of Korea; [4]Department of Biomaterial Science, Pusan National University, Miryang, Kyungnam, Republic of Korea and [5]Department of Bioscience and Biotechnology, Bio/Molecular Informatics Center, Konkuk University, Gwangjin-gu, Seoul, Republic of Korea. Correspondence: Professor JT Hong, College of Pharmacy and Medical Research Center, Chungbuk National University, 48 Gaeshin-dong, Heungduk-gu, Cheongju, 361-763, Chungbuk, Republic of Korea.
E-mail: jinthong@chungbuk.ac.kr
[6]The authors contributed equally to this work.
Received 9 January 2014; revised 11 April 2014; accepted 14 April 2014; published online 26 May 2014

sarcoidosis.[32] We previously found that iPLA2 activity is critical for lung tumor development in *in vivo* allograft.[33] Moreover, it was observed that lung tumor growth was significantly lowered in the PS- mutant mice compared with non-transgenic mice through a decrease of iPLA2 activity with increased γ-secretase activity (data not shown). It was found that tumor progression of glioblastoma and lewis lung carcinoma were more regressed in $PLA2^{-/-}$ mice than $PLA2^{+/+}$ mice. Interestingly, the active site of the PLA2 is GXSXG at positions 30–34, which has been termed a phospholipase motif.[34,35] This phospholipase motif could be cleaved by γ-secretase, leading to the inhibition of phospholipase activity. Therefore, we hypothesized that the ablation of PS2 could have a critical role in lung cancer development via an increase of iPLA2 activity of PRDX6 via the reduction of γ-secretase activity.

RESULTS

Promotion of lung tumor growth in PS2 knockout mice

Previously, we found that lung tumor growth was lower in PS2 (N141I)-mutant transgenic mice than that of PS2 wild-type mice or non-transgenic mice (unpublished data). Therefore, we were interested in studying the effect of PS2 knockout on lung cancer development. To determine whether PS2 knockout contributes to lung tumorigenesis, lung tumorigenesis was induced using urethane injections. Thirty weeks after the initial urethane injections, a significantly increased number of lung tumors in knockout mice was found. The number of lung tumors in PS2 knockout mice were significantly increased (Figure 1a). Tumor multiplicity was 40.3 ± 7.5 tumors per PS2 knockout mice, but 15.9 ± 5.7 per PS2 wild-type mice. The histological findings after haematoxylin and eosin staining indicated that the tumors in PS2 knockout mice were well-differentiated lung adenomas; however, tumors from PS2 wild-type mice were significantly smaller than those from PS2 knockout mice, and showed a few adenocarcinoma (Figure 1b, upper panel). The percentage of PCNA-positive cells was higher in PS2 knockout mice ($61.2 \pm 2.3\%$, $^{**}P < 0.01$) than PS2 wild-type mice (Figure 1b, lower panel). As shown in Supplementary Figure 1, we exhibited the pictures of normal lung tissues and the lung tissues were stained with haematoxylin and eosin. We also detected the PCNA to evaluate proliferative activity in the normal lung tissues. As a result, there is no difference between the normal lung tissues of PS2 knockout mice and PS2 wild-type mice. Western blotting data also showed that the protein levels of PCNA, Ki67, MMP2, MMP9, cyclin B, cyclin D1, cyclin E, cyclin-dependent kinase 1 (Cdk1), Cdk2, Cdk4 and Cdk6 were significantly increased in the tumor tissues of the PS2 knockout mice than in the wild-type mice, and also we observed that p-pRb was increased in the PS2 knockout mice, leading to a malignant phenotype by functional loss of pRb (Figure 1c and Supplementary Figure 2).

Inactivation of γ-secreatase increases activities of iPLA2 and GPx, and protein levels of iPLA2 cleavage and PRDX6 in tumor tissue

PRDX6 is known to be critical for lung tumor growth, and its expression is elevated in the lung tumor patients.[33] Therefore, we determined whether the expression of PRDX6 is increased in the lung tumor tissue of PS2 knockout mice. To quantify the expression of PRDX6 in a variety of tissues of PS2 knockout mice and wild-type mice, PRDX6 expression was investigated by western blots. Higher expression of PRDX6 was found in the tumor tissues of PS2 knockout mice compared with that of the tumor tissues of wild-type mice (Figure 2a). PRDX6 has glutathione peroxidase and iPLA2 activities which are important in lung tumor growth. To confirm the relative glutathione peroxidase and iPLA2 activities in the tumor tissue of PS2 knockout mice and wild-type mice, we investigated glutathione peroxidase and iPLA2 activities assay. Associated with the increase of tumor growth, glutathione peroxidase and iPLA2 activities in lung tumor tissues of PS2

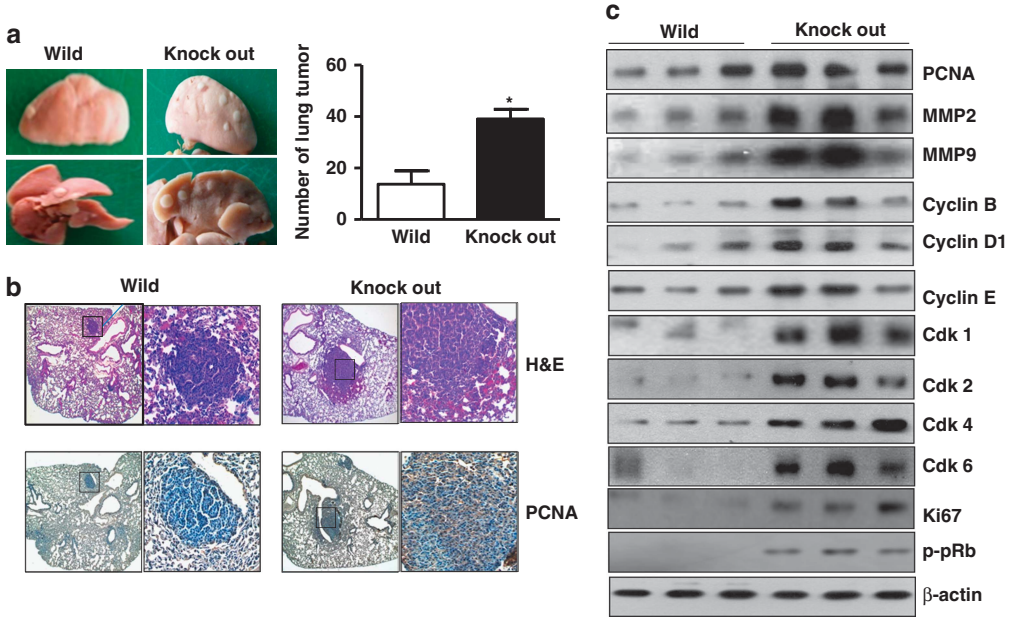

Figure 1. Effect of PS2 knockout on the development of lung tumor. (**a**) Tumors were induced by a single intraperitoneal injection of 1 mg/g urethane once a week for 10 weeks. Mice were euthanized at time points up to 6 months after injection of carcinogen. At the time of killing, lungs were lavaged, perfused and fixed in ice-cold Bouin's fixative solution for 24 h. After fixation, lungs were used for surface tumor number and diameter measurements. The results are expressed as mean ± s.d. (**b**) Lung tissues were processed and stained with haematoxylin and eosin or analyzed by immunohistochemistry for detection of positive cells for PCNA. (**c**) Tumor extracts were analyzed by western blotting. Samples (20 μg) were resolved on SDS–PAGE, and detected with antibodies against PCNA, MMP2, MMP9, Cyclin (B, D1 and E), Cdk (1, 2, 4 and 6), Ki67, p-pRb and β-actin. The experiments shown in Figure 1 were repeated in triplicate with similar results. $^{*}P < 0.05$ compared with the wild-type mice.

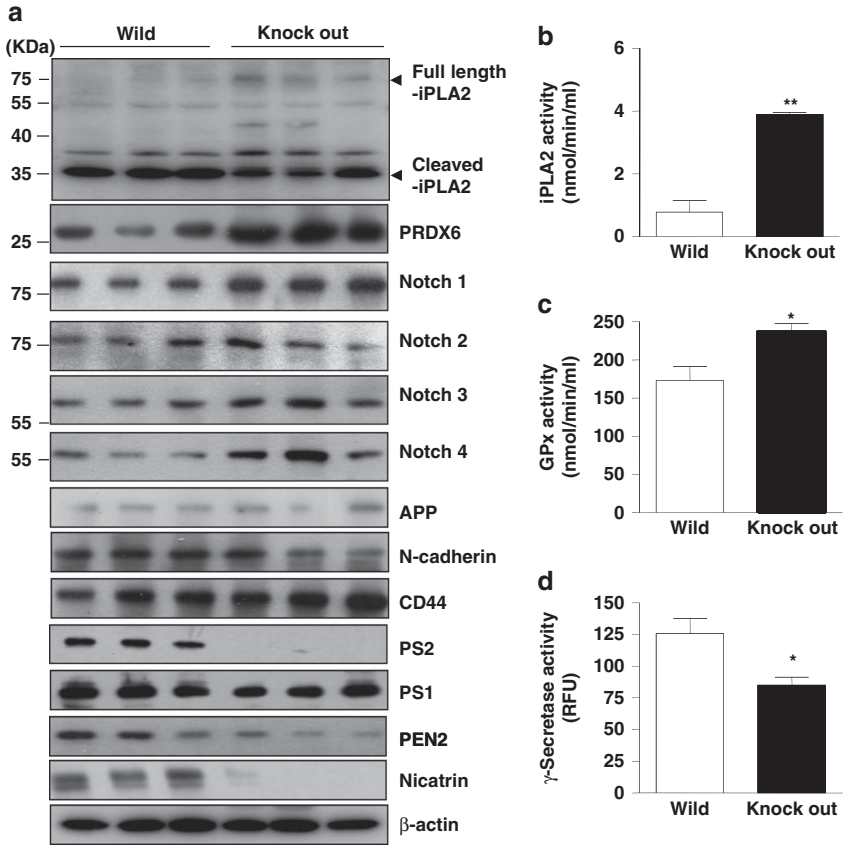

Figure 2. Effect of PS2 knockout on the cleavage of iPLA2, the expression of PRDX6, and activates. (**a**) Tumor extracts were analyzed by western blotting. Samples (20 μg) were resolved on SDS–PAGE and detected with antibodies against Notch (1, 2, 3 and 4), APP, N-cadherin, CD44, iPLA2, PRDX6, PS2, PS1, PEN2, Nicastrin and β-actin. (**b**, **c**) The levels of iPLA2 (**b**) and glutathione peroxidase (**c**) activities were measured in lung tumor tissues using assay kits, as described in Materials and methods. (**d**) The level of γ-secretase activity was measured in lung tumor tissues of urethane-induced wild-type mice and PS2 knockout mice as described in Materials and methods. $*P < 0.05$ and $**P < 0.01$, significant difference from the wild-type mice. The experiments shown in Figure 2 were repeated in triplicate with similar results.

knockout mice were much higher than in the tumor of wild-type mice (Figures 2b and c). The phospholipase motif (GXSXG) is the catalytic site of PLA2, which is significantly affected by the γ-secretase.[36] Thus, we determined γ-secreatase activity in the lung tumor tissues. We found that γ-secretase activity was statistically lowered in lung tumor tissues of PS2 knockout mice (Figure 2d). This result indicated that loss of PS2 could affect γ-secretase in tumor tissues, causing enhancing or keeping of iPLA2 activity. The PS/γ-secretase complex cleaves several other substrates such as APP, notch, CD44 and N-cadherin which have GXXXG pentapeptide domain. Since iPLA2 has GXGXG motif site in phospholipase active site, it could be cleaved by γ-secretase. Thus, we determined the cleavage of iPLA2 in the lung tumor tissues of PS2 knockout mice. Compared with the lung tumor tissues of wild-type mice, the cleavage form of iPLA2 (35 KDa cleaved form) was significantly lowered in lung tumor tissues of PS2 knockout mice. However, there was little difference (even slightly higher in Notch-1 and 4, and CD44) in the cleavage of other substrates such as Notch-1–4, APP, N-cadherin and CD44 between the lung tumor tissues of PS2 knockout mice and wild-type mice (Figure 2a and Supplementary Figures 3 and 4). We also detected the expression levels of different components of the γ-Secretase complex in lung tumor tissues of PS2 knockout mice, and we found that the γ-secretase complex was decreased in PS2 knockout mice but not PS1 (Figure 2a and Supplementary Figure 4). As shown in Supplementary Figure 5, we additionally detected the Notch-1–4, APP, PRDX6, p-pRb, MMP2 and components of the γ-secretase complex in the normal lung tissues. As a result, there are no differences between the normal lung tissues of PS2 knockout mice and PS2 wild-type mice, except for PRDX6.

Increase of NF-κB, AP-1 and STAT3 activities in tumor tissue of PS2 knockout mice

The activation of nuclear factor kappa-beta (NF-κB), AP-1 and STAT3 has a critical role in tumor growth. Moreover, NF-κB and AP-1 are located in the promoter region of iPLA2 and PRDX6 genes. To evaluate whether the promotion of lung tumor development was related with the activation of these transcriptional factors in the urethane-treated mice, the DNA-binding activity of NF-κB, STAT3 and AP-1 was determined by an electromobility shift assay in the lung tissue. The higher DNA-binding activity of NF-κB, STAT3 and AP-1 was found in the lung tissues of PS2 knockout mice compared with that of wild-type mice (Figures 3a and c). We also performed antibody supershift studies and validated the band of NF-κB, STAT3 and AP-1 in electromobility shift assay data (data not shown). Since NF-κB is translocated from cytosol into nucleus to play a role as a transcriptional regulator, which is induced by the phosphorylation of IκB, we investigated the translocation p50 and p65 of NF-κB using immunohistochemistry analysis. As shown in Figure 3d, the intensity of nuclear staining for p65 and p50 was increased in the lung tissues of PS2 knockout mice. Moreover, we confirmed that the increase of the translocation of p50 and p65 into the nucleus through an increase of the phosphorylation of IκB was also observed in PS2 knockout mice lung tissues (Figure 3e). The

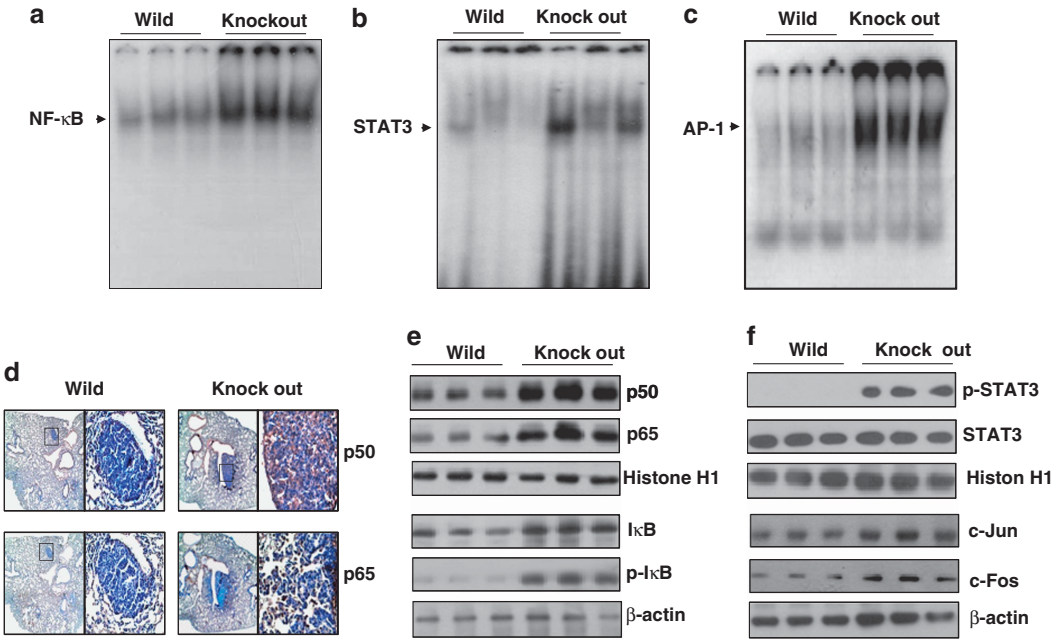

Figure 3. Effect of PS2 knockout on the activation of NF-κB, STAT3 and AP-1, and their DNA-binding activities in urethane-induced lung tumors. (**a**–**c**) DNA-binding activity of NF-κB (**a**), STAT3 (**b**) and AP-1 (**c**) in the lung tumor tissues was determined by electromobility shift assay in nuclear extracts as described in Materials and methods. (**d**) Lung tissues were processed and analyzed by immunohistochemistry for detection of positive cells for p50 and p65. (**e**, **f**) Tumor extracts were analyzed by western blotting. Samples (20 μg) were resolved on SDS–PAGE and detected with antibodies against p50, p65, IkB and p-IkB (**e**), and p-STAT3, STAT3, c-Jun and c-Fos (**f**). β-actin and Histone H1 were used as cytosol marker and nucleus marker, respectively. The experiments shown in Figure 3 were repeated in triplicate with similar results.

higher c-Fos, c-Jun and p-STAT3 expression in nucleus was also found in PS2 knockout mice lung tissues (Figure 3f). We also found that tumor expression levels of IL-6 were increased in the lung tumors of PS2 Knoctout mice compared with wild-type mice (Supplementary Figure 6).

Promoting function of loss of PS2 in γ-secretase and lung cancer cell growth

To further investigate whether the loss of PS2 inhibits γ-secretase activity and has an enhancing effect on lung cancer cell growth through increasing iPLA2 activity, we knockdowned PS2 using PS2 siRNA in lung cancer cells (A549 and NCI-H460). We found that γ-secretase activity was significantly decreased in the lung cancer cells transfected with siRNA of PS2 (Figures 4a and b). However, lung cancer cell growth was increased by the knockdown of PS2 (Figures 4c and d). With the increase of lung cancer cell growth, iPLA2 activity was elevated by knockdown of PS2 (Figures 4e and f). We also found the expression of full length of iPLA2 and the expression of PRDX6 in the lung cancer cells transfected with siRNA of PS2 were significantly higher than those of the lung cancer cells transfected with control siRNA (Figures 4g and h). Similar to tumor tissues, NF-κB (Figures 5a and b), STAT3 (Figures 5c and d) and AP-1 (Figures 5e and f) DNA-binding activity were also increased by knockdown of PS2 in lung cancer cells.

DISCUSSION

In this study, we have shown that the knockout of PS2 significantly elevated the development of carcinogen-induced lung tumor. Consistent with the increase of lung tumor development, the expression of PRDX6 and iPLA2 activity were significantly increased, but γ-secretase activity was significantly decreased in the lung tumor tissues of PS2 knockout mice compared with the PS2 wild-type mice. Much higher activity of iPLA2, higher DNA-binding activities, and expression of subunits of NF-κB, STAT3 and AP-1, as well as PCNA, MMPs, Cyclins and CDKs were found in the lung tumor tissue of PS2 knockout mice. We also found that PS2 siRNA transfection significantly decreased γ-secretase activity, but significantly elevated cancer cell growth in accordance with the increase of iPLA2 in culture lung cancer cells. The present data suggest that PS2 is essential in carcinogen-induced lung tumor growth via decreased γ-secretase in PS2 knockout mice.

In lung cancer cells and lung tumor patients, the expression of PRDX6 is elevated and the expression of PRDX6 in lung tumor is critical for tumor progression, and resistance for apoptotic cell death.[32] PRDX6 has two enzyme activities such as glutathione peroxidase and iPLA2 activities.[31] The elevation of these two enzyme activities are related with the enhancement of cholangiocarcinoma growth and human lung cancer cells, and the probability of relapse including lung metastases and local recurrences.[37–39] The activation of iPLA2 also contributes to lung metastasis and stimulates the invasion of A549 and H460 human lung cancer cells.[40,41] Lewis lung carcinoma grows much faster in iPLA2$^{-/-}$ mice than in IPLA2$^{+/+}$ mice. We recently found that PRDX6 overexpressed Tg mice also promoted lung tumor development through upregulation of iPLA2.[33] In the present study, we found that PS2 knockout increased PRDX6 expression and iPLA2 activities accompanied with increased lung tumor and lung cancer cell growth. Thus, the elevation of iPLA2 activity could be significant in promoting the effect of lung tumor development in PS2 knockout mice. The increased activity of iPLA2 in lung tumor tissues of carcinogen-inducted PS2 knockout mice correlated significantly with the overexpression of PCNA, MMP2 and MMP9. Therefore, the higher activity of iPLA2 by PS2 knockout may be significant in the regulation of genes involved in cell proliferation, metastasis and angiogenesis, leading to an increase in lung tumor development in PS2 knockout mice. However, the exact mechanism(s) of how the loss of PS2 could influence iPLA2 activity is (are) not clear.

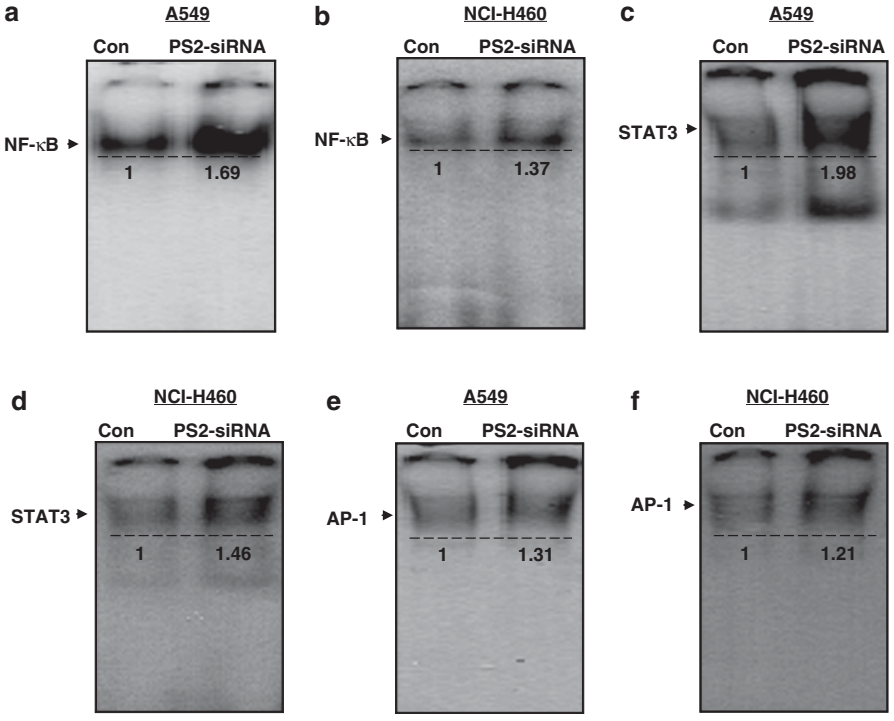

Figure 4. Effect of PS2 knockdown on DNA-binding activities of NF-κB, STAT3 and AP-1 in lung cancer cells. After control siRNA and PS2 siRNA were transfected in A549 and NCI-H460 cell, DNA-binding activity of NF-κB (**a**, **b**), STAT3 (**c**, **d**) and AP-1 (**e**, **f**) in the lung cancer cells was determined by electromobility shift assay in nuclear extracts as described in Materials and methods. The experiments shown in Figure 4 were repeated in triplicate with similar results.

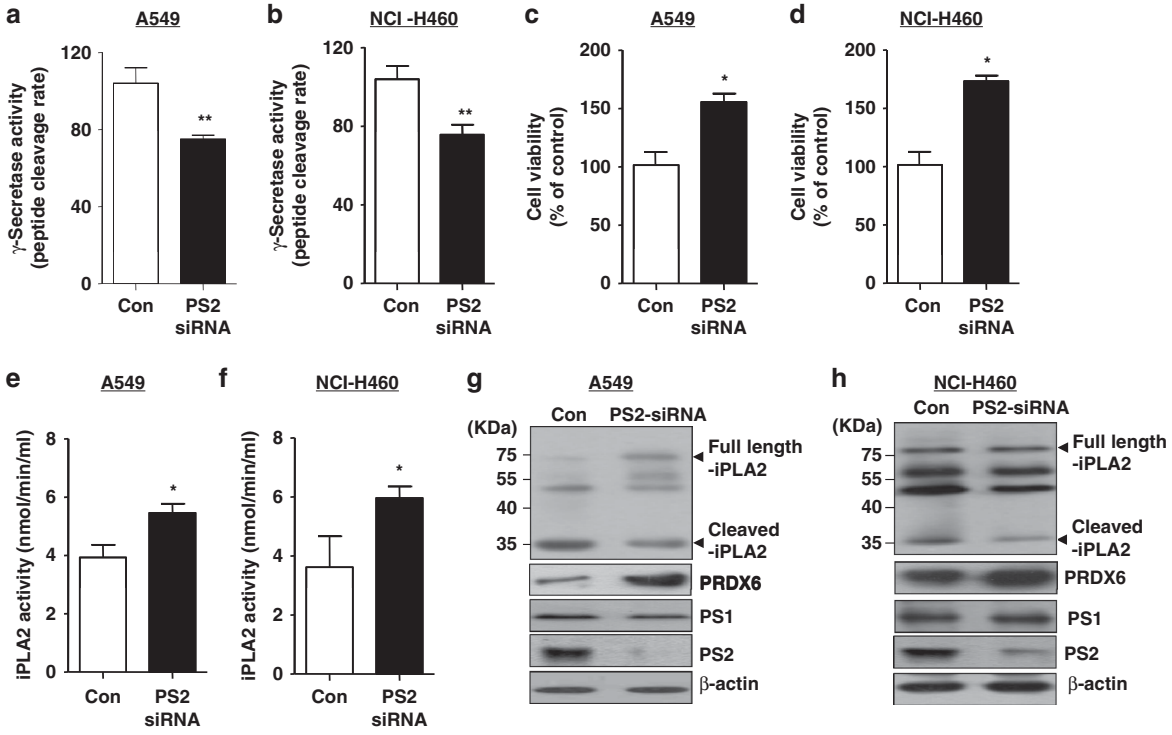

Figure 5. Effect of PS2 knockdown on cell viability, the cleavage of iPLA2, the expression of PRDX6 and activates. (**a**, **b**) A549 (**a**) and NCI-H460 (**b**) (1×106) were transfected with control siRNA and PS2 siRNA for 48 h, and then γ-secretase activity was detected. (**c**, **d**) After A549 (**c**) and NCI-H460 (**d**) cells were cultured in 96-well plates (1×104 cells per well) and transfected with control siRNA and PS2 siRNA for 48 h, cell viability was analyzed by MTT assay. (**e**, **f**) The levels of iPLA2 activities were measured in A549 (**e**) and NCI-H460 (**f**) transfected with control siRNA and PS2 siRNA for 48 h. (**g**, **h**) A549 cell lysates (**g**) and NCI-H460 cell lysates (**h**) were analyzed by western blotting. Samples (20 μg) were resolved on SDS–PAGE, and detected with antibodies against iPLA2, PRDX6, PS1, PS2 and β-actin. All values are presented as the mean ±s.e.m. $^{*}P < 0.05$ and $^{**}P < 0.01$, significant difference from the control. The experiments shown in Figure 5 were repeated in triplicate with similar results.

PS is the essential core component of γ-secretase, an enzymatic complex composed of PS, nicastin, anterior pharynx-defective phenotype-1 and PS enhancer-2.[3] It is known that the mutation of PSs could enhance γ-secretase activity causing an increase of amyloid beta peptide production by cleavage from APP.[2,5] γ-secretase cleavages notably membrane proteins such as APP but also other proteins such as N- and E-cadherin, Notchs and CD44 which have GxxxG, conserved motif.[7] It is noteworthy that PRDX6 could be a substrate of γ-secretase. Since phospholipase motif (GXSXG) is in the catalytic site of iPLA2 in PRDX6, and this GXXXG site is the helix-dimerization motif significantly affected by the property of the γ-secretase substrate. The iPLA2 activity was decreased by cleavage with γ-secretase in the wild-type PS2 mice, but PS2 knockout mice maintained iPLA2 activity since γ-secretase activity was lowered by the deletion of PS2. Our data also showed that the higher γ-secretase activity was found in lung cancer cells, and the cleavage of iPLA2 was increased. However, the γ-secretase activity was lowered by knockdown of PS2 and the lower γ-secretase activity maintained iPLA2 activity. It was also found that higher iPLA2 activity was associated with the growth of lung cancer cells in PS2 siRNA-transfected lung cancer cells. Thus, it can be speculated that an increase of the cleavage of iPLA2 by γ-secretase at the phospholipase motif site of iPLA2 in PRDX6 causes a decrease in iPLA2 activity in wild-type PS2 mice lung, but not in PS2 knockout mice lung. We previously found that iPLA2 activity is critical for lung tumor development in *in vivo* allograft and xenograft mice model.[33,42] Moreover, it was observed that lung tumor growth was significantly lowered in the PS2-mutant mice compared with non-transgenic mice through the decrease of iPLA2 activity with increased γ-secretase activity (data not shown). These data thus suggest that the maintenance of iPLA2 activity in PS2 knockout mice by loss of γ-secretase activity could promote carcinogen-induced tumor growth.

Other mechanisms could be possible. PS/γ-secretase-generated amyloid precursor protein intracellular domain mediates transcriptional regulation of the epidermal growth factor receptor by directly binding with epidermal growth factor receptor promoter, which results in the skin and glioma tumor-promoting effect.[43] PS/γ-secretase-dependent cleavages of oncoprotein Notch also contributed to the development of tumor.[12] Cleavages and nuclear translocation of E-cadherin by PS/γ-secretase increased metastasis of colorectal cancer.[44] PS/γ-secretase-dependent cleavages and nuclear translocation of CD44 are also involved in glioma growth.[45] However, in the PS2 knockout and wild-type lung tumor tissues treated with carcinogen, the cleavages of other substrates such as APP, cadherin, Notch-1 and CD44 was not significantly changed. This data, thus, demonstrate that iPLA2 rather than Notchs, APP, cadherin and CD44 could be significant in the carcinogen-induced lung tumor development in PS2 knockout mice. In addition, although two homologs, PS1 and PS2, have some specific biological functions, we found that the PS2 knockout mice did not affect PS1 expression compared with wild-type mice. Thus, in our experimental models, these findings indicate that the tumor development increased in PS2 knockout mice is specifically mediated by PS2. Taken together, our data show that the loss of PS/γ-secretase-dependent cleavages of iPLA2 promotes lung tumor development via the maintenance of iPLA2 activity, and also we speculate that the specific regulation for iPLA2 of PS2 in the carcinogen-induced lung tumor model may give us a way to underline controversial roles of PS/γ-secretase based on existing data in the literature.

NF-κB, STAT3 and AP-1 are also involved in the cell proliferation, metastasis and angiogenesis through regulation of tumor-promoting genes such as PCNA, MMP, Cyclins and Cdks.[46] In the present study, western blotting revealed that the expression of PCNA, MMPs, Cyclins and Cdks was higher in the tumors of PS2 knockout mice lung tumor tissues compared with the tumor tissues of wild-type PS2 mice lung. NF-κB, STAT3 and AP-1 activities were also much higher in the lung tumor tissues of PS2 knockout mice compared with those of the lung tumor of wild-type PS2 mice. Moreover, consistent with the upregulation of iPLA2 activities, PS2 siRNA increased NF-κB, STAT3 and AP-1 activates in lung cancer cells accompanied with increased cancer cell growth. Therefore, a higher level of AP-1, NF-κB and STAT3 activates in tumor tissue of PS2 knockout mice may be also significant in the carcinogen-induced lung tumor growth by upregulation of genes involved in cell proliferation, metastasis and angiogenesis. Even though these transcriptional factors are significant in lung tumor development, it is not clear whether the activation of these transcriptional factors could be caused by increased tumor development, increased iPLA2 or increased expression of PRDX6. On the contrary, the activation of these transcriptional factors contributed to iPLA2 activity, and then promoted tumor development, since these transcriptional factors are located in the promoting regions of iPLA2 or PRDX6 genes.[33,47] In conclusion, the present data conclusively indicate that PS2 could be significant in the lung tumor development by modulation of iPLA2 through change of γ-secretase.

MATERIALS AND METHODS

Animals

The PS2 knockout mice were purchased from the Jackson Laboratory (Bar Harbor, ME, USA). The genetic background of wild type and PS2 knockout mice is C57BL/6. The mice were housed and bred under specific pathogen-free conditions at the Laboratory Animal Research Center of Chungbuk National University, Korea (CBNUA-436-12-02). The mice ($n = 15$) were maintained in a room with a constant temperature of 22 ± 1 °C, relative humidity of $55 \pm 10\%$ and 12-h light/dark cycle and fed standard rodent chow (Samyang, Gapyeong, Korea) and purified tap water *ad libitum*.

Carcinogenesis protocols

Eighteen to twenty-week-old mice were used. Tumors were induced by a single intraperitoneal injection of 1 mg/g urethane (ethyl carbamate; Sigma-Aldrich, St Louis, MO, USA) once a week for 10 weeks. Mice were euthanized at time points up to 6 months after injection of carcinogen. At the time of sacrifice, lungs were lavaged, perfused and fixed in ice-cold Bouin's fixative solution (Sigma-Aldrich) for 24 h. After fixation, lungs were used for surface tumor number and diameter measurements, and embedded in paraffin. Tumors on the lung surface were enumerated by at least two experienced readers, blinded to sample identifiers under a dissecting microscope; tumor counts were averaged and statistically analyzed. Tumor diameters were measured using Fisherbrand Traceable digital calipers (Fisher Scientific, Ashville, NC, USA).

Glutathione peroxidase activity and iPLA2 activity assay

Glutathione peroxidase assay and PLA2 assay kit were purchased from Cayman Chemical (Biomol GmbH, Hamburg, Germany). iPLA2 activities and glutathione peroxidase activities according to the manufacturer's recommendations (Cayman Chemical). GPx co-substrate mixture including nicotinamide adenine dinucleotide phosphate, glutathione and glutathione reductase was used to measure glutathione peroxidase activity *in vitro*. Arachidonoyl thio-PC was used as the substrate to measure total PLA2 activity and PLA2 activity excluding other iPLA2 activities using the iPLA2 inhibitor, bromoenol lactone because bromoenol lactone does not inhibit iPLA2 activity of PRDX6,[48] instead of MJ33 (a specific inhibitor for iPLA2 activity of PRDX6) *in vitro*, and then iPLA2 activity was determined by subtracting the rate PLA2 excluding iPLA2 from rate of total PLA2. Briefly, after treatment of cells or perfusing tissue with a phosphate-buffered saline (PBS) buffer, the cells or tissue were homogenized. Supernatants in a total volume of 45 μl were added to microplate wells containing 5 μl of assay buffer with or without 10 μM bromoenol lactone. The reaction was initiated by addition of 200 μl of arachidonoyl thio-PC and was incubated at room temperature for 60 min. The reaction was terminated by addition of 10 μl of 25 mM 5,5′-dithio-bis(2-nitrobenzoic acid), and the absorbance was measured at 405 nm. The iPLA2 activity was calculated according to the manufacturer's instructions.

Immunohistochemistry

All specimens were fixed in formalin and paraffin-enclosed for examination. The sections were blocked for 30 min with 3% normal horse serum diluted in PBS. The sections were then blotted and incubated with specific primary antibodies (1:200 dilution) at the appropriate dilution in blocking serum for 4 h at room temperature at the appropriate dilution in blocking serum for overnight at 4 °C. The next day, the slides were washed three times for 5 min each in PBS and incubated in biotinylated anti-mouse and rabbit antibody for 2 h. The slides were washed in PBS, followed by formation of the avidinbiotin-peroxidase complex (ABC, Vector Laboratories, Burlingame, CA, USA). The slides were washed and the peroxidase reaction developed with diaminobenzidine and peroxide, then counterstained with hematoxylin, mounted in aqua-mount, and evaluated using a light microscope (×200, Olympus, Tokyo, Japan).

Western blot analysis

The membranes were immunoblotted with primary specific antibodies. The blot was then incubated with corresponding conjugated anti-rabbit and anti-mouse immunoglobulin G-horseradish peroxidase (1:2000 dilution, Santa Cruz Biotechnology, Santa Cruz, CA, USA). Immunoreactive proteins were detected with the enhanced chemiluminescence (ECL) western blotting detection system. The intensity of the bands was measured using the Fusion FX 7 image acquisition system (Vilber Lourmat, Eberhardzell, Germany).

γ-secretase assay

Enzyme activity levels were quantified using an assay kit based on the description by Farmery *et al*.[49]

Electromobility shift assay

Briefly, 1×10^6 cells/ml were washed twice with 1 × PBS, followed by the addition of 1 ml of PBS and then cells were scraped into a cold Eppendorf tube. Cells were spun down at 15 000 *g* for 1 min and the resulting supernatant was removed. Solution A (50 mM 4-(2-hydroxyethyl)-1-piperazineethanesulfonic acid, pH 7.4, 10 mM KCl, 1 mM ethylenediaminetetraacetic acid, 1 mM ethylene glycol tetraacetic acid, 1 mM dithiothreitol, 0.1 μg/ml phenylmethylsulfonyl fluoride, 1 μg/ml pepstatin A, 1 μg/ml leupeptin, 10 μg/ml soybean trypsin inhibitor, 10 μg/ml aprotinin and 0.5% Nonidet P-40) was added to the pellet in a 2:1 ratio (v/v) and incubated on ice for 10 min. In total, 0.5 g of tumor tissue was chopped into 1.5 ml of solution A. The tumor pieces were then homogenized and centrifuged at 12 000 *g* for 15 min at 4 °C. Solution C (solution A+10% glycerol and 400 mM KCl) was added to the pellet in a 2:1 ratio (v/v) and vortexed on ice for 20 min. After centrifugation at 15 000 *g* for 7 min, the resulting nuclear extract supernatant was collected in a chilled Eppendorf tube. Consensus oligonucleotides, AP-1, NF-κB and STAT3 (Promega corporation, Madison, WI, USA), were end-labeled using T4 polynucleotide kinase and (γ -32P) ATP for 10 min at 37 °C. Gel shift reactions were assembled and allowed to incubate at room temperature for 10 min followed by the addition of 1 μl (50 000–200 000 c.p.m.) of ^{32}P-labeled oligonucleotide and another 20 min of incubation at room temperature. Subsequently, 1 μl of gel-loading buffer was added to each reaction and loaded onto a 4% nondenaturing gel and electrophoresed until the dye was 75% of the way down the gel. The gel was dried at 80 °C for 1 h and exposed to film overnight at 70 °C. The intensity of the bands was measured using the Fusion FX 7 image acquisition system (Vilber Lourmat, Eberhardzell, Germany).

Cell culture

NCI-H460 and A549 human lung cancer cells were obtained from the American Type Culture Collection (Manassas, VA, USA). RPMI1640, penicillin, streptomycin and fetal bovine serum were purchased from Invitrogen (Carlsbad, CA, USA). Both cells were grown in RPMI1640 with 10% fetal bovine serum, 100 U/ml penicillin and 100 μg/ml streptomycin at 37 °C in 5% CO_2 humidified air.

Transfection

Lung cancer cells were transiently transfected with control and PS2 siRNA (Santa Cruz Biotechnology) using the WelFect-EX PLUS reagent in OPTI-MEN, according to the manufacturer's specification (WelGENE, Seoul, Korea).

Cell viability assay

For 3-[4,5-dimethylthiazol-2-yl]-2,5 diphenyl tetrazolium bromide (MTT) assay, 10% vol/vol of 5 mg/ml 3-(4,5-dimethylthiazol-2-yl)-2,5-diphenyltetrazolium bromide (MTT; Sigma, St Louis MO, USA) diluted in PBS was added to A549 and NCI-H460 cell cultures. After 2 h of incubation, the medium was aspirated and dimethlysulfoxide was added. Absorbance was measured at 570 nm. The data were normalized to their respective controls and are presented as a bar graph.

Enzyme-linked immunosorbent assay

For the detection of IL-6 level, lung tumor tissues were analyzed using Mouse IL-6 ELISA Kit (Cusabio Biotech, China).

Data analysis

The data were analyzed using the GraphPad Prism 4 ver. 4.03 software (GraphPad Software, La Jolla, CA, USA). Data are presented as mean ± s.d. The differences in all data were assessed by one-way analysis of variance. When the *P*-value in the analysis of variance test indicated statistical significance, the differences were assessed by the Dunnett's test. A value of $P < 0.05$ was considered to be statistically significant.

CONFLICT OF INTEREST

The authors declare no conflict of interest.

ACKNOWLEDGEMENTS

This work was supported by the National Research Foundation of Korea (NRF) grant funded by the Korea Government (MSIP) (No; MRC, 2008-0062275).

REFERENCES

1 Bertram L, Lill CM, Tanzi RE. The genetics of Alzheimer disease: back to the future. *Neuron* 2010; **68**: 270–281.
2 Kovacs DM, Fausett HJ, Page KJ, Kim TW, Moir RD, Merriam DE *et al.* Alzheimer-associated presenilins 1 and 2: neuronal expression in brain and localization to intracellular membranes in mammalian cells. *Nat Med* 1996; **2**: 224–229.
3 De Strooper B. Aph-1, Pen-2, and Nicastrin with Presenilin generate an active gamma-Secretase complex. *Neuron* 2003; **38**: 9–12.
4 De Strooper B, Annaert W. Novel research horizons for presenilins and gamma-secretases in cell biology and disease. *Annu Rev Cell Dev Biol* 2010; **26**: 235–260.
5 Wakabayashi T, De Strooper B. Presenilins: members of the gamma-secretase quartets, but part-time soloists too. *Physiology (Bethesda)* 2008; **23**: 194–204.
6 Boulton ME, Cai J, Grant MB. gamma-Secretase: a multifaceted regulator of angiogenesis. *J Cell Mol Med* 2008; **12**: 781–795.
7 Beel AJ, Sanders CR. Substrate specificity of gamma-secretase and other intramembrane proteases. *Cell Mol Life Sci* 2008; **65**: 1311–1334.
8 Murakami D, Okamoto I, Nagano O, Kawano Y, Tomita T, Iwatsubo T *et al.* Presenilin-dependent gamma-secretase activity mediates the intramembranous cleavage of CD44. *Oncogene* 2003; **22**: 1511–1516.
9 Park CS, Kim OS, Yun SM, Jo SA, Jo I, Koh YH. Presenilin 1/gamma-secretase is associated with cadmium-induced E-cadherin cleavage and COX-2 gene expression in T47D breast cancer cells. *Toxicol Sci* 2008; **106**: 413–422.
10 Liu B, Wang L, Shen LL, Shen MZ, Guo XD, Wang T *et al.* RNAi-mediated inhibition of presenilin 2 inhibits glioma cell growth and invasion and is involved in the regulation of Nrg1/ErbB signaling. *Neuro Oncol* 2012; **14**: 994–1006.
11 Rahimi N, Golde TE, Meyer RD. Identification of ligand-induced proteolytic cleavage and ectodomain shedding of VEGFR-1/FLT1 in leukemic cancer cells. *Cancer Res* 2009; **69**: 2607–2614.
12 Das I, Craig C, Funahashi Y, Jung KM, Kim TW, Byers R *et al.* Notch oncoproteins depend on gamma-secretase/presenilin activity for processing and function. *J Biol Chem* 2004; **279**: 30771–30780.
13 Kang DE, Soriano S, Xia X, Eberhart CG, De Strooper B, Zheng H *et al.* Presenilin couples the paired phosphorylation of beta-catenin independent of axin: implications for beta-catenin activation in tumorigenesis. *Cell* 2002; **110**: 751–762.
14 Tarassishin L, Yin YI, Bassit B, Li YM. Processing of Notch and amyloid precursor protein by gamma-secretase is spatially distinct. *Proc Natl Acad Sci USA* 2004; **101**: 17050–17055.
15 Rocher-Ros V, Marco S, Mao JH, Gines S, Metzger D, Chambon P *et al.* Presenilin modulates EGFR signaling and cell transformation by regulating the ubiquitin ligase Fbw7. *Oncogene* 2010; **29**: 2950–2961.

16 Xia X, Qian S, Soriano S, Wu Y, Fletcher AM, Wang XJ *et al.* Loss of presenilin 1 is associated with enhanced beta-catenin signaling and skin tumorigenesis. *Proc Natl Acad Sci USA* 2001; **98**: 10863–10868.
17 Serrano J, Fernandez AP, Martinez-Murillo R, Martinez A. High sensitivity to carcinogens in the brain of a mouse model of Alzheimer's disease. *Oncogene* 2010; **29**: 2165–2171.
18 To MD, Gokgoz N, Doyle TG, Donoviel DB, Knight JA, Hyslop PS *et al.* Functional characterization of novel presenilin-2 variants identified in human breast cancers. *Oncogene* 2006; **25**: 3557–3564.
19 Song X, Xia R, Cui Z, Chen W, Mao L. Presenilin 1 is frequently overexpressed and positively associates with epidermal growth factor receptor expression in head and neck squamous cell carcinoma. *Head Neck Oncol* 2012; **4**: 47.
20 Kovacs DM, Mancini R, Henderson J, Na SJ, Schmidt SD, Kim TW *et al.* Staurosporine-induced activation of caspase-3 is potentiated by presenilin 1 familial Alzheimer's disease mutations in human neuroglioma cells. *J Neurochem* 1999; **73**: 2278–2285.
21 Tanii H, Ankarcrona M, Flood F, Nilsberth C, Mehta ND, Perez-Tur J *et al.* Alzheimer's disease presenilin-1 exon 9 deletion and L250S mutations sensitize SH-SY5Y neuroblastoma cells to hyperosmotic stress-induced apoptosis. *Neuroscience* 2000; **95**: 593–601.
22 Roe CM, Behrens MI, Xiong C, Miller JP, Morris JC. Alzheimer disease and cancer. *Neurology* 2005; **64**: 895–898.
23 Takahashi T. Lung cancer: an ever increasing store of in-depth basic knowledge and the beginning of its clinical application. *Oncogene* 2002; **21**: 6868–6869.
24 Thun MJ, Hannan LM, Adams-Campbell LL, Boffetta P, Buring JE, Feskanich D *et al.* Lung cancer occurrence in never-smokers: an analysis of 13 cohorts and 22 cancer registry studies. *PLoS Med* 2008; **5**: e185.
25 Liu Y, Chen Q, Zhang JT. Tumor suppressor gene 14-3-3sigma is down-regulated whereas the proto-oncogene translation elongation factor 1delta is up-regulated in non-small cell lung cancers as identified by proteomic profiling. *J Proteome Res* 2004; **3**: 728–735.
26 Zhang XZ, Xiao ZF, Li C, Xiao ZQ, Yang F, Li DJ *et al.* Triosephosphate isomerase and peroxiredoxin 6, two novel serum markers for human lung squamous cell carcinoma. *Cancer Sci* 2009; **100**: 2396–2401.
27 Granville CA, Dennis PA. An overview of lung cancer genomics and proteomics. *Am J Respir Cell Mol Biol* 2005; **32**: 169–176.
28 Wood WJ, Huang L, Ellman JA. Synthesis of a diverse library of mechanism-based cysteine protease inhibitors. *J Comb Chem* 2003; **5**: 869–880.
29 Lehtonen ST, Svensk AM, Soini Y, Paakko P, Hirvikoski P, Kang SW *et al.* Peroxiredoxins, a novel protein family in lung cancer. *Int J Cancer* 2004; **111**: 514–521.
30 Olahova M, Taylor SR, Khazaipoul S, Wang J, Morgan BA, Matsumoto K *et al.* A redox-sensitive peroxiredoxin that is important for longevity has tissue- and stress-specific roles in stress resistance. *Proc Natl Acad Sci USA* 2008; **105**: 19839–19844.
31 Kim SY, Chun E, Lee KY. Phospholipase A(2) of peroxiredoxin 6 has a critical role in tumor necrosis factor-induced apoptosis. *Cell Death Differ* 2011; **18**: 1573–1583.
32 Schremmer B, Manevich Y, Feinstein SI, Fisher AB. Peroxiredoxins in the lung with emphasis on peroxiredoxin VI. *Subcell Biochem* 2007; **44**: 317–344.
33 Jo M, Yun HM, Park KR, Hee Park M, Myoung Kim T, Ho Pak J *et al.* Lung tumor growth-promoting function of peroxiredoxin 6. *Free Radic Biol Med* 2013; **61C**: 453–463.
34 Sagi SA, Lessard CB, Winden KD, Maruyama H, Koo JC, Weggen S *et al.* Substrate sequence influences gamma-secretase modulator activity, role of the transmembrane domain of the amyloid precursor protein. *J Biol Chem* 2011; **286**: 39794–39803.
35 Borgegard T, Jureus A, Olsson F, Rosqvist S, Sabirsh A, Rotticci D *et al.* First and second generation gamma-secretase modulators (GSMs) modulate amyloid-beta (Abeta) peptide production through different mechanisms. *J Biol Chem* 2012; **287**: 11810–11819.
36 Munter LM, Voigt P, Harmeier A, Kaden D, Gottschalk KE, Weise C *et al.* GxxxG motifs within the amyloid precursor protein transmembrane sequence are critical for the etiology of Abeta42. *EMBO J* 2007; **26**: 1702–1712.
37 Chen F, Hasegawa H, Schmitt-Ulms G, Kawarai T, Bohm C, Katayama T *et al.* TMP21 is a presenilin complex component that modulates gamma-secretase but not epsilon-secretase activity. *Nature* 2006; **440**: 1208–1212.
38 Wang L, Chanvorachote P, Toledo D, Stehlik C, Mercer RR, Castranova V *et al.* Peroxide is a key mediator of Bcl-2 down-regulation and apoptosis induction by cisplatin in human lung cancer cells. *Mol Pharmacol* 2008; **73**: 119–127.
39 Conti A, Rodriguez GC, Chiechi A, Blazquez RM, Barbado V, Krenacs T *et al.* Identification of potential biomarkers for giant cell tumor of bone using comparative proteomics analysis. *Am J Pathol* 2011; **178**: 88–97.
40 McHowat J, Gullickson G, Hoover RG, Sharma J, Turk J, Kornbluth J. Platelet-activating factor and metastasis: calcium-independent phospholipase A2beta deficiency protects against breast cancer metastasis to the lung. *Am J Physiol Cell Physiol* 2011; **300**: C825–C832.
41 Oh S, Kim Y, Kim J, Kwon D, Lee E. Elevated pressure, a novel cancer therapeutic tool for sensitizing cisplatin-mediated apoptosis in A549. *Biochem Biophys Res Commun* 2010; **399**: 91–97.
42 Yun HM, Park KR, Lee HP, Lee DH, Jo M, Shin DH *et al.* PRDX6 promotes lung tumor progression via its GPx and iPLA2 activities. *Free Radic Biol Med* 2014; **69C**: 367–376.
43 Zhang W, Weissfeld JL, Romkes M, Land SR, Grandis JR, Siegfried JM. Association of the EGFR intron 1 CA repeat length with lung cancer risk. *Mol Carcinog* 2007; **46**: 372–380.
44 Cespedes MV, Larriba MJ, Pavon MA, Alamo P, Casanova I, Parreno M *et al.* Site-dependent E-cadherin cleavage and nuclear translocation in a metastatic colorectal cancer model. *Am J Pathol* 2010; **177**: 2067–2079.
45 Liu HY, Wen ZP, Wen M, He HR, Tan SD, Li SL. Effects of magnetic c-erbB-2 antisense probe of different concentrations on morphology and expression of SK-Br-3 cancer cell lines *in vitro*. *Zhongguo Yi Xue Ke Xue Yuan Xue Bao* 2013; **35**: 19–23.
46 Yan KX, Liu BC, Shi XL, Zhang XM, You BR, Xu M *et al.* The role of cycline dependent kinase 4 in the malignant transformation induced by silica. *Zhonghua Lao Dong Wei Sheng Zhi Ye Bing Za Zhi* 2004; **22**: 331–335.
47 Chhunchha B, Fatma N, Kubo E, Rai P, Singh SP, Singh DP. Curcumin abates hypoxia-induced oxidative stress based-ER stress-mediated cell death in mouse hippocampal cells (HT22) by controlling Prdx6 and NF-kappaB regulation. *Am J Physiol Cell Physiol* 2013; **304**: C636–C655.
48 Chatterjee S, Feinstein SI, Dodia C, Sorokina E, Lien YC, Nguyen S *et al.* Peroxiredoxin 6 phosphorylation and subsequent phospholipase A2 activity are required for agonist-mediated activation of NADPH oxidase in mouse pulmonary microvascular endothelium and alveolar macrophages. *J Biol Chem* 2011; **286**: 11696–11706.
49 Farmery MR, Tjernberg LO, Pursglove SE, Bergman A, Winblad B, Naslund J. Partial purification and characterization of gamma-secretase from post-mortem human brain. *J Biol Chem* 2003; **278**: 24277–24284.

Supplementary Information accompanies this paper on the Oncogene website (http://www.nature.com/onc)